Aligned Channel Estimation for Beamforming Design in IRS-assisted MIMO Communications

Yuri S. Ribeiro, André L. F. de Almeida, Fazal E-Asim

***Abstract*— In this paper, we analyze three different methods to perform channel estimation aligned with the joint active and passive beamforming design in an intelligent reflecting surface (IRS)-assisted multiple input multiple output (MIMO) networks. For this purpose, we explore the Kronecker structure of the involved channels to factorize each channel in horizontal and vertical channel components. After the factorized channels are estimated, we apply different strategies to active and passive beamforming designs where each method apply different strategies to jointly optimize the active and passive beamforming. Simulation results showed that the methods which explore the Kronecker structure can significantly enhance the spectral efficiency compared to the benchmark model, due to the processing done to obtain the factorized channel components which reduces the noise from the channel estimation step, with less computational complexity.**

***Keywords*— channel factorization, channel estimation, intelligent reflecting surface, beamforming, MIMO.**

I. Introduction

Intelligent reflecting surface (IRS) is regarded as a promising technology to be used in beyond fifth generation (B5G) due to its capability to enhance the system performance by creating a virtual line-of-sight (LoS) link between the base station (BS) and the user-equipment (UE) which can, for example, increase the data rate without adding radio-frequency chains [1], [2]. The IRS is a uniform rectangular array (URA) composed of several reflecting elements and each element is capable of reflecting the impinging wave with different phases in order to generate a construct interference at the UE. In the context of terahertz (THz) communications, the IRS can create a virtual LoS link between the BS and the UE and reduce the attenuation losses related to high frequencies [3]. On the other hand, by adding the IRS into the wireless network a new channel has to be estimated, the BS to the IRS channel. Since the IRS is usually a passive structure it does not have signal processing capability making the channel estimation step more challenging and in order to adjust the reflecting elements both channels or the composed channel, i.e., end-to-end channel, must be estimated. In this context, the works of [4] and [5] proposed a channel estimation using an on-off scheme of different groups of reflecting elements. In practice, the off-stage is an ideal scenario since it considers that the reflecting elements are capable of acting as perfect absorber. To overcome that issue, [6] proposed a DFT-based scheme where the IRS phase shifts are given according to a column of the DFT matrix. In [7] and [8], the authors used the DFT scheme to obtain the composed channel via a least squares (LS) strategy and then proposed a Khatri-Rao factorization (KRF) to estimate the BS-IRS channel and the IRS-UE channel. regarding IRS-assisted THz communications, the works of [9] and [10] explored the Kronecker structure in the geometrical channel model to perform a high-order tensor decomposition to estimate the angles of arrival and departure.

Regarding the joint beamforming design of active beamforming, precoder and combiner, at the BS and the UE, respectively, and passive beamforming, IRS phase shifts, in [11], the authors proposed singular value decomposition (SVD)-based solutions to jointly optimize the precoder, combiner, and IRS phase shifts. In [12], the authors explored the Kronecker structure in the geometrical channel to split the beamforming optimization problem into horizontal and vertical sub-problems to maximize the received SNR at the UE.

The aforementioned works did not study the impact of the channel estimation techniques aligned with the joint active and passive beamforming design, considering the Kronecker structure of the channels. In this regard, this paper studies the impact of different channel estimation procedures in the joint active and passive beamforming design by comparing the spectral efficiency (SE) achieved by each method as well as their computational complexities. Our results show the trade-offs involved by the different methods.

Notation: Scalars, vector, matrices and tensors are denoted (a), $(\boldsymbol{a})$, $(\boldsymbol{A})$ and $(\mathcal{A})$, respectively. The superscripts $\{\}^T$, $\{\}^*$, $\{\}^\dagger$ and $\{\}^H$ denote transpose, conjugate, pseudo-inverse, and hermitian, respectively. The operators $\otimes$, $\diamond$, $\circ$, $\odot$ and $\angle$ are the Kronecker, the Khatri-Rao, the outer product, the Hadamard products, and the angle of a complex value, respectively. $\text{vec}(\boldsymbol{A})$ converts $\boldsymbol{A}$ to a column vector by stacking its columns. The n-mode product of a tensor $\mathcal{X} \in \mathbb{C}^{I\times J\times K}$ and a matrix $\boldsymbol{A} \in \mathbb{C}^{I\times R}$ is denoted by $\mathcal{Y} = \mathcal{X} \times_n \boldsymbol{A}$, $n = 1, 2, 3$.

II. System Model

In this paper, we consider an IRS-assisted multiple input multiple output (MIMO) system, where the BS utilizes M antennas to transmit towards an UE with L antennas, through an IRS that features N reflecting elements. Additionally, there is no direct link between the BS and the UE.

A. Least Square (LS) Channel Estimation

In order to estimate the combined channel a time-slotted transmission is used. During the channel training, we consider K blocks with T time slots each totaling TK time slots to

This work was partially supported by the Brazilian National Council for Scientific and Technological Development (CNPq), the Coordenação de Aperfeiçoamento de Pessoal de Nível Superior - Brasil (CAPES) - Finance Code 001, in part by CNPq 306845/2020-2, and Fundação Cearense de Apoio ao Desenvolvimento Científico e Tecnológico (FUNCAP) - Grant FC3-00198-00056.01.00/22.

perform the channel estimation. During the k-th block $k \in [1, \dots, K]$ the IRS phase shifts are constant, and during the t-th time slot $t \in [1, \dots, T]$ the pilots transmitted are constant. In this case, the IRS phase shifts only vary with k and the pilots only vary with t. Both pilot sequence and IRS phase shifts are respectively given by the columns of a $T \times T$ and $K \times K$ DFT matrices. The signal received by the UE, at the k-th block and t-th time slot, can be expressed as

$$\boldsymbol{r}[k,t] = \boldsymbol{G}\text{diag}(\boldsymbol{s}[k])\boldsymbol{H}\boldsymbol{x}[t] + \boldsymbol{z}[k,t], \tag{1}$$

where $\boldsymbol{G} \in \mathbb{C}^{L\times N}$ is the channel between the IRS and the UE, $\boldsymbol{s}[k] \in \mathbb{C}^N$ is the IRS phase shift vector at the k block defined as $\boldsymbol{s} \doteq [s_1, \dots, s_N]^T$ with $\angle[s_n] \in [-\pi, \pi)$ representing the phase shift of the n-th reflecting element and the reflection amplitude is $|s_n| = 1$, $\boldsymbol{H} \in \mathbb{C}^{N\times M}$ is the channel between the BS and the IRS, $\boldsymbol{x}[t] \in \mathbb{C}^{M\times 1}$ is the pilot symbol at the t-th time slot with power P_t and $\boldsymbol{z}[k,t] \in \mathbb{C}^{L\times 1}$ is the additive white Gaussian noise (AWGN) vector with zero mean and σ_z^2 variance. By collecting the received signal during one block we can write the received signal at the k-th block as

$$\boldsymbol{R}[k] = \boldsymbol{G}\text{diag}(\boldsymbol{s}[k])\boldsymbol{H}\boldsymbol{X} + \boldsymbol{Z}[k], \tag{2}$$

where $\boldsymbol{R}[k] \doteq [\boldsymbol{r}[k,1], \dots, \boldsymbol{r}[k,T]] \in \mathbb{C}^{L\times T}$, $\boldsymbol{X} \doteq [\boldsymbol{x}[1], \dots, \boldsymbol{x}[T]] \in \mathbb{C}^{M\times T}$ and $\boldsymbol{Z}[k] \doteq [\boldsymbol{z}[k,1], \dots, \boldsymbol{z}[k,T]] \in \mathbb{C}^{L\times T}$. After this, we can apply a matched filter with the pilot knowledge and the filtered received signal at the k-th block can be written as

$$\boldsymbol{R}[k]\boldsymbol{X}^\dagger = \boldsymbol{G}\text{diag}(\boldsymbol{s}[k])\boldsymbol{H} + \boldsymbol{Z}'[k], \tag{3}$$

where $\boldsymbol{Z}'[k] = \boldsymbol{Z}[k]\boldsymbol{X}^\dagger$ is the filtered noise term. We can apply $\text{vec}(\boldsymbol{A}\text{diag}(\boldsymbol{b})\boldsymbol{C}) = (\boldsymbol{C}^T \diamond \boldsymbol{A})\boldsymbol{b}$ in (3) to obtain

$$\boldsymbol{r}[k] = (\boldsymbol{H}^T \diamond \boldsymbol{G})\boldsymbol{s}[k] + \boldsymbol{z}'[k] \tag{4}$$

where $\boldsymbol{r}[k] \doteq \text{vec}(\boldsymbol{R}[k]) \in \mathbb{C}^{LT\times 1}$ and $\boldsymbol{z}'[k] \doteq \text{vec}(\boldsymbol{Z}'[K]) \in \mathbb{C}^{LT\times 1}$. By concatenating $\boldsymbol{r}[k]$ during the K blocks the received signal during the channel training procedure can be written as

$$\boldsymbol{R} = (\boldsymbol{H}^T \diamond \boldsymbol{G})\boldsymbol{S} + \boldsymbol{Z}', \tag{5}$$

where $\boldsymbol{R} \doteq [\boldsymbol{r}[1], \dots, \boldsymbol{r}[K]] \in \mathbb{C}^{LT\times K}$, $\boldsymbol{S} \doteq [\boldsymbol{s}[1], \dots, \boldsymbol{s}[K]] \in \mathbb{C}^{N\times K}$, $\boldsymbol{Z}' \doteq [\boldsymbol{z}'[1], \dots$ and $\boldsymbol{z}'[K]] \in \mathbb{C}^{LT\times K}$. The composed channel is defined as $\boldsymbol{F} \doteq \boldsymbol{H}^T \diamond \boldsymbol{G}$.

Finally, to obtain an estimation of the composed channel we apply a right filter in (5) with the knowledge of the IRS phase shifts during the channel training stage

$$\hat{\boldsymbol{F}} = \boldsymbol{R}\boldsymbol{S}^\dagger. \tag{6}$$

As discussed in [7] the LS estimate of $\boldsymbol{F}$ is given by (6). In order to estimate $\boldsymbol{F}$, the number of blocks and time slots must obey $K \geq N$ and $T \geq M$.

B. Single Stage: Khatri-Rao Factorization (KRF)

Furthermore, with an estimation of the composed channel $\boldsymbol{F}$ is possible to obtain the estimations of $\boldsymbol{H}$ and $\boldsymbol{G}$ since the composed channel is given by the Khatri-Rao product of those channels. The estimations of $\boldsymbol{H}$ and $\boldsymbol{G}$ can be obtained through the KRF which solves the following optimization problem (further details can be found in [7])

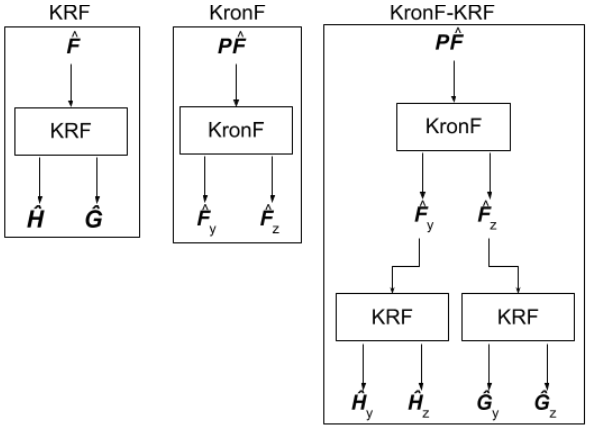

Fig. 1: Diagram of the channel estimation methods

$$\min_{\hat{\boldsymbol{H}},\hat{\boldsymbol{G}}} ||\hat{\boldsymbol{F}} - \hat{\boldsymbol{H}}^T \diamond \hat{\boldsymbol{G}}||_F^2. \tag{7}$$

After the KRF step in (7) we have $\hat{\boldsymbol{H}} = \boldsymbol{H}\text{diag}(\boldsymbol{\alpha}_H)$ and $\hat{\boldsymbol{G}} = \boldsymbol{G}\text{diag}(\boldsymbol{\alpha}_G)$, where $\boldsymbol{\alpha}_H, \boldsymbol{\alpha}_G \in \mathbb{C}^{N\times 1}$ are the vectors containing the scaling factors that are inherent to the KRF procedure, such that $\text{diag}(\boldsymbol{\alpha}_H)\text{diag}(\boldsymbol{\alpha}_G) = \boldsymbol{I}_N$.

III. Two-Dimensional Channel Estimation

In this paper, we consider that both BS and UE antennas consist of URA. The BS is equipped with M_y antennas along the y axis and M_z along the z axis where $M = M_y M_z$. Similarly, the UE is equipped with L_y and L_z antennas along the y and z axis respectively, where $L = L_y L_z$. The IRS is also assumed to be an URA with N_y and N_z reflecting elements along the y and z axis, respectively, with $N = N_y N_z$. According to [12] if we consider the geometrical channel model and the channel has only one path, i.e., LoS channel, then this channel can be written as a Kronecker product of its horizontal and vertical components. In this case, the channels $\boldsymbol{H}$ and $\boldsymbol{G}$ can be written as

$$\boldsymbol{H} = \boldsymbol{H}_y \otimes \boldsymbol{H}_z \quad \boldsymbol{G} = \boldsymbol{G}_y \otimes \boldsymbol{G}_z, \tag{8}$$

where $\boldsymbol{H}_y \in \mathbb{C}^{N_y\times M_y}$ and $\boldsymbol{H}_z \in \mathbb{C}^{N_z\times M_z}$ are the horizontal and vertical components of $\boldsymbol{H}$, respectively, and also, $\boldsymbol{G}_y \in \mathbb{C}^{L_y\times N_y}$ and $\boldsymbol{G}_z \in \mathbb{C}^{L_z\times N_z}$ are the horizontal and vertical components of $\boldsymbol{G}$ respectively. If more paths are assumed the expressions in (8) become approximations. The impacts of these approximations are discussed in Section VI.

A. Single Stage: Kronecker Factorization (KronF)

By considering the Kronecker structure of the channels in (8), the composed channel $\boldsymbol{F}$ can be written as

$$\boldsymbol{F} = (\boldsymbol{H}_y \otimes \boldsymbol{H}_z)^T \diamond (\boldsymbol{G}_y \otimes \boldsymbol{G}_z). \tag{9}$$

It is possible to rewrite (9) using the property $(\boldsymbol{A} \otimes \boldsymbol{B}) \diamond (\boldsymbol{C} \otimes \boldsymbol{D}) = \boldsymbol{P}\,[(\boldsymbol{A} \diamond \boldsymbol{C}) \otimes (\boldsymbol{B} \diamond \boldsymbol{D})]$, where $\boldsymbol{P}$ is a permutation matrix defined in [9]

$$\boldsymbol{P}\boldsymbol{F} = (\boldsymbol{H}_y^T \diamond \boldsymbol{G}_y) \otimes (\boldsymbol{H}_z^T \diamond \boldsymbol{G}_z). \tag{10}$$

We define $\boldsymbol{F}_y \doteq (\boldsymbol{H}_y^T \diamond \boldsymbol{G}_y)$ and $\boldsymbol{F}_z \doteq (\boldsymbol{H}_z^T \diamond \boldsymbol{G}_z)$ to be the horizontal and vertical composed channel components, respectively. In order to estimate $\boldsymbol{F}_y$ and $\boldsymbol{F}_z$, we transform the estimated composed channel matrix obtained in (6) by means of the row-permutation matrix $\boldsymbol{P}$, which allows us to formulate a Kronecker factorization (KronF) problem as follows (details can be found in [8]):

$$\min_{\hat{\boldsymbol{F}}_y, \hat{\boldsymbol{F}}_z} ||\boldsymbol{P}\hat{\boldsymbol{F}} - \hat{\boldsymbol{F}}_y \otimes \hat{\boldsymbol{F}}_z||_F^2. \tag{11}$$

After the KronF in (11) we have $\hat{\boldsymbol{F}}_y = \gamma_y \boldsymbol{F}_y$ and $\hat{\boldsymbol{F}}_y = \gamma_z \boldsymbol{F}_z$, where $\gamma_y, \gamma_z \in \mathbb{C}$ are the scaling factors inherent to the KronF procedure, such that $\gamma_y \gamma_z = 1$.

B. Two Stage: Kronecker and Khatri-Rao Factorization (Kron-KRF)

After the KronF stage in (11) we can explore the Khatri-Rao structure in $\boldsymbol{F}_y$ and $\boldsymbol{F}_z$ to obtain $\boldsymbol{G}_y, \boldsymbol{G}_z, \boldsymbol{H}_y, \boldsymbol{H}_z$. To estimate the horizontal channel components, the KRF method is applied in $\hat{\boldsymbol{F}}_y$, solving the following problem

$$\min_{\hat{\boldsymbol{H}}_y, \hat{\boldsymbol{G}}_y} ||\hat{\boldsymbol{F}}_y - \hat{\boldsymbol{H}}_y^T \diamond \hat{\boldsymbol{G}}_y||_F^2. \tag{12}$$

Similarly, the vertical channel components are estimated by applying the KRF method to $\hat{\boldsymbol{F}}_z$, which solves the following problem

$$\min_{\hat{\boldsymbol{H}}_z, \hat{\boldsymbol{G}}_z} ||\hat{\boldsymbol{F}}_z - \hat{\boldsymbol{H}}_z^T \diamond \hat{\boldsymbol{G}}_z||_F^2. \tag{13}$$

Solving problems (12) and (13) provide us with $\hat{\boldsymbol{H}}_y = \boldsymbol{H}_y \text{diag}(\boldsymbol{\alpha}_{Hy})$, $\hat{\boldsymbol{H}}_z = \boldsymbol{H}_z \text{diag}(\boldsymbol{\alpha}_{Hz})$, $\hat{\boldsymbol{G}}_y = \boldsymbol{G}_y \text{diag}(\boldsymbol{\alpha}_{Gy})$ and $\hat{\boldsymbol{G}}_z = \boldsymbol{G}_z \text{diag}(\alpha_{Gz})$, where these diagonal matrices contain the scaling ambiguity factors, such that $\text{diag}(\boldsymbol{\alpha}_{Hy})\text{diag}(\boldsymbol{\alpha}_{Gy}) = \boldsymbol{I}_N$ and $\text{diag}(\boldsymbol{\alpha}_{Hz})\text{diag}(\boldsymbol{\alpha}_{Gz}) = \boldsymbol{I}_N$.

It is worth noting that the vertical and horizontal channel components can not be directly obtained from the estimated channel matrices $\hat{\boldsymbol{H}}$ and $\hat{\boldsymbol{G}}$ due to the KRF scaling ambiguities that break the model of (8). In this case, the scaling ambiguities of $\hat{\boldsymbol{H}}$ and $\hat{\boldsymbol{G}}$ would have to be separable, i.e., they would have to satisfy $\text{diag}(\boldsymbol{\alpha}) = \text{diag}(\boldsymbol{\alpha}_1) \otimes \text{diag}(\boldsymbol{\alpha}_2)$. Such an assumption is not possible since $\boldsymbol{\alpha}$ is a random vector that does not follow a Kronecker (separable) structure.

Fig 1 presents a diagram of the steps involved in each channel estimation method.

IV. Beamforming Design

In this section, we will detail the different beamforming design methods associated with each channel estimation procedure. In this regard, the received signal at the UE is given by

$$r = \boldsymbol{w}^H \hat{\boldsymbol{G}} \text{diag}(\boldsymbol{s}) \hat{\boldsymbol{H}} \boldsymbol{q} x + a, \tag{14}$$

where $\boldsymbol{w} \in \mathbb{C}^{L \times 1}$ is the combiner vector, $\boldsymbol{q} \in \mathbb{C}^{M \times 1}$ is the precoder vector, $x \in \mathbb{C}$ is the transmitted symbol with power P and a is the AWGN with $a \sim \mathcal{CN}(0, \sigma_a^2)$.

Algorithm 1: Classical solution [11]

1 Compute the truncated SVD of $\boldsymbol{G}$ and $\boldsymbol{H}$ $\lambda_{\text{g}} \boldsymbol{u}_{\text{g}} \boldsymbol{v}_{\text{g}}^H \approx \boldsymbol{G}$ and $\lambda_{\text{h}} \boldsymbol{u}_{\text{h}} \boldsymbol{v}_{\text{h}}^H \approx \boldsymbol{H}$.
2 Design the combiner as $\boldsymbol{w} = \boldsymbol{u}_{\text{g}}$.
3 Design the precoder as $\boldsymbol{q} = \boldsymbol{v}_{\text{h}}$.
4 Design the IRS phase shifts as $\boldsymbol{s} = -\angle[\boldsymbol{v}_{\text{g}}^* \odot \boldsymbol{u}_{\text{h}}]$

A. Classical solution

In this regard, we want to maximize the received signal by adjusting the precoder, combiner, and IRS phase shifts properly using the channel estimations obtained from the single-stage: KRF. This leads to the following optimization problem

$$\begin{aligned} &\max_{\boldsymbol{w}, \boldsymbol{q}, \boldsymbol{s}} |(\boldsymbol{w}^H \hat{\boldsymbol{G}} \text{diag}(\boldsymbol{s}) \hat{\boldsymbol{H}} \boldsymbol{q})|^2 \\ &\text{s.t. } ||\boldsymbol{w}|| = ||\boldsymbol{q}|| = 1 \text{ and } s_n \in [-\pi, \pi]. \end{aligned} \tag{15}$$

A solution to this problem was proposed by [11]. The solution relies on rank one approximation of the channels $\boldsymbol{H}$ and $\boldsymbol{G}$ to obtain the dominant eigenvectors which are used to design the precoder, combiner, and IRS phase shifts. The steps to solve the beamforming optimization are presented in Algorithm 1.

B. Kronecker Factorized (KF) solution

By considering the channel components obtained in III-A, it is possible to rewrite (14) as the product of the horizontal and vertical received signal if we impose a Kronecker structure on the precoder, combiner, and IRS phase shifts vectors, i.e., $\boldsymbol{w} \doteq \boldsymbol{w}_y \otimes \boldsymbol{w}_z, \boldsymbol{q} \doteq \boldsymbol{q}_y \otimes \boldsymbol{q}_z$ and $\boldsymbol{s} \doteq \boldsymbol{s}_y \otimes \boldsymbol{s}_z$. This leads to

$$r = d_y d_z + a, \tag{16}$$

where $d_y \doteq \boldsymbol{w}_y^H \hat{\boldsymbol{G}}_y \text{diag}(\boldsymbol{s}_y) \hat{\boldsymbol{H}}_y \boldsymbol{q}_y$ is the horizontal desired signal and $d_z \doteq \boldsymbol{w}_z^H \hat{\boldsymbol{G}}_z \text{diag}(\boldsymbol{s}_z) \hat{\boldsymbol{H}}_z \boldsymbol{q}_z$ is the vertical desired signal. In this case, we can also write the SNR as a product between horizontal and vertical SNR, respectively given by $\text{SNR}_y \doteq |d_y|^2 / \sqrt{\sigma_a^2}$ and $\text{SNR}_z \doteq |d_z|^2 / \sqrt{\sigma_a^2}$. This means that maximizing the SNR is the same as individually maximizing SNR_y and SNR_z. In this regard, [12] proposed the KF method which solves the problem in (15) by maximizing SNR_y and SNR_z as follows

$$\begin{aligned} &\max_{\boldsymbol{w}_y, \boldsymbol{q}_y, \boldsymbol{s}_y} |(\boldsymbol{w}_y^H \hat{\boldsymbol{G}}_y \text{diag}(\boldsymbol{s}_y) \hat{\boldsymbol{H}}_y \boldsymbol{q}_y)|^2 \\ &\text{s.t. } ||\boldsymbol{w}_y|| = ||\boldsymbol{q}_y|| = 1 \text{ and } \boldsymbol{s}_y \in [-\pi, \pi], \end{aligned} \tag{17}$$

$$\begin{aligned} &\max_{\boldsymbol{w}_z, \boldsymbol{q}_z, \boldsymbol{s}_z} |(\boldsymbol{w}_z^H \hat{\boldsymbol{G}}_z \text{diag}(\boldsymbol{s}_z) \hat{\boldsymbol{H}}_z \boldsymbol{q}_z)|^2 \\ &\text{s.t. } ||\boldsymbol{w}_z|| = ||\boldsymbol{q}_z|| = 1 \text{ and } \boldsymbol{s}_z \in [-\pi, \pi]. \end{aligned} \tag{18}$$

To solve the problems in (17) and (18) the classical method, detailed in Section IV-A, is used in each domain then the horizontal and vertical beamforming vectors are combined *via* a Kronecker product. This procedure is summarized in Alg. 2.

Algorithm 2: KF solution [12]

1 Compute the truncated SVD of $\boldsymbol{G}_y$, $\boldsymbol{G}_z$, $\boldsymbol{H}_y$ and $\boldsymbol{H}_z$. $\lambda_{\mathrm{g}_y}\boldsymbol{u}_{\mathrm{g}_y}\boldsymbol{v}_{\mathrm{g}_y}^H \approx \boldsymbol{G}_y$, $\lambda_{\mathrm{g}_z}\boldsymbol{u}_{\mathrm{g}_z}\boldsymbol{v}_{\mathrm{g}_z}^H \approx \boldsymbol{G}_z$, $\lambda_{\mathrm{h}_y}\boldsymbol{u}_{\mathrm{h}_y}\boldsymbol{v}_{\mathrm{h}_y}^H \approx \boldsymbol{H}_y$ and $\lambda_{\mathrm{h}_z}\boldsymbol{u}_{\mathrm{h}_z}\boldsymbol{v}_{\mathrm{h}_z}^H \approx \boldsymbol{H}_z$.
2 Design the combiner as $\boldsymbol{w} = \boldsymbol{u}_{\mathrm{g}_y} \otimes \boldsymbol{u}_{\mathrm{g}_z}$.
3 Design the precoder as $\boldsymbol{q} = \boldsymbol{v}_{\mathrm{h}_y} \otimes \boldsymbol{v}_{\mathrm{h}_z}$.
4 Design the IRS phase shifts as $\boldsymbol{s} = -\angle\{[\boldsymbol{v}_{\mathrm{g}_y}^* \odot \boldsymbol{u}_{\mathrm{h}_y}] \otimes [\boldsymbol{v}_{\mathrm{g}_z} \odot \boldsymbol{u}_{\mathrm{h}_z}]\}$

C. Third-Order Tensor (TOT) solution

In this section, we detail the beamforming optimization associated with the single stage: KronF. In this context, the Khatri-Rao structure in $\hat{\boldsymbol{F}}_y$ and $\hat{\boldsymbol{F}}_z$ can be directly used to solve the beamforming problem in (15). This is possible by rearranging $\hat{\boldsymbol{F}}_y$ and $\hat{\boldsymbol{F}}_z$ as third-order tensors using the following mapping $[\mathcal{F}_y]_{l_y,m_y,n_y} \doteq [\boldsymbol{F}_y]_{(l_y-1)M_y+m_y,n_y}$ and $[\mathcal{F}_z]_{l_z,m_z,n_z} \doteq [\boldsymbol{F}_z]_{(l_z-1)M_z+m_z,n_z}$, where $\mathcal{F}_y \in \mathbb{C}^{L_y \times M_y \times N_y}$ and $\mathcal{F}_z \in \mathbb{C}^{L_z \times M_z \times N_z}$, $l_t = 1,\ldots,L_t$, $m_t = 1,\ldots,M_t$, $n_t = 1,\ldots,N_t$, $t \in \{y,z\}$. Considering this tensor formulation, the desired signal d_y and d_z can be written as $d_y = \mathcal{F}_y \times_1 \boldsymbol{w}_y \times_2 \boldsymbol{q}_y \times_3 \boldsymbol{s}_y$ and $d_z = \mathcal{F}_z \times_1 \boldsymbol{w}_z \times_2 \boldsymbol{q}_z \times_3 \boldsymbol{s}_z$. Similarly to the KF solution, we want to maximize d_y and d_z, but now considering the tensor modeling which leads to the following optimization problems

$$\max_{\boldsymbol{w}_y,\boldsymbol{q}_y,\boldsymbol{\theta}_y} ||\hat{\mathcal{F}}_y \times_1 \boldsymbol{w}_y \times_2 \boldsymbol{q}_y \times_3 \boldsymbol{s}_y||^2 \quad (19)$$
$$\text{s.t. } ||\boldsymbol{w}_y|| = ||\boldsymbol{q}_y|| = 1 \text{ and } s_y \in [-\pi,\pi]$$

$$\max_{\boldsymbol{w}_z,\boldsymbol{q}_z,\boldsymbol{\theta}_z} ||\hat{\mathcal{F}}_z \times_1 \boldsymbol{w}_z \times_2 \boldsymbol{q}_z \times_3 \boldsymbol{s}_z||^2 \quad (20)$$
$$\text{s.t. } ||\boldsymbol{w}_z|| = ||\boldsymbol{q}_z|| = 1 \text{ and } s_z \in [-\pi,\pi]$$

To solve these problems two independent high order singular value decomposition (HOSVD) can be applied in $\hat{\mathcal{F}}_y$ and $\hat{\mathcal{F}}_z$ (a detailed explanation about the HOSVD is given in [13]). The horizontal combiner, precoder, and IRS phase shifts $(\boldsymbol{w}_y, \boldsymbol{q}_y, \boldsymbol{s}_y)$ are respectively given by the dominant left singular vector of the first mode, second mode and third mode of $\mathcal{F}_y$ and the same procedure is done in $\mathcal{F}_z$ to obtain the vertical combiner, precoder, and IRS phase shifts. The steps involved in the TOT solution [12] are detailed in Alg. 3.

Algorithm 3: TOT solution [12]

1 Compute the HOSVD of $\mathcal{F}_y$ and $\mathcal{F}_z$ to obtain $\{\boldsymbol{w}_y, \boldsymbol{q}_y, \boldsymbol{\theta}_y\}$ and $\{\boldsymbol{w}_z, \boldsymbol{q}_z, \boldsymbol{\theta}_z\}$, respectively.
2 Design the combiner as $\boldsymbol{w} = \boldsymbol{w}_y \otimes \boldsymbol{w}_z$.
3 Design the precoder as $\boldsymbol{q} = \boldsymbol{q}_y^* \otimes \boldsymbol{q}_z^*$.
4 Design the IRS phase shifts as $\boldsymbol{s} = -\angle[\boldsymbol{s}_y \otimes \boldsymbol{s}_z]$.

V. Computational Complexity

Let us recall all the steps involved in each method to equate the computational complexity of each method, since the LS is common for all of them it is disregarded. Since all the methods are based on rank one approximations, according to [14], this operation has a complexity of $O(IJ)$, where I is the number of columns and J is the number of lines. The complexities of the KRF and the KronF are the same and are given by the rank one approximation of the matrix which is being factorized. The complexities of the beamforming solutions are given by the rank one approximation of each estimated channel component.

The complexity of the single stage: KRF is given by $O[NML]$ and the complexity of the classical beamforming design is $O[N(M+L)]$. The overall complexity is $O[N(ML+M+L)]$.

The complexity of the double stage: KronF-KRF is given by $O[NML + M_yL_yN_y + M_zL_zN_z]$ and the complexity of the KF beamforming design is $O[N_y(M_y+L_y)+N_z(M_z+L_z)]$. The resulting complexity is $O[MNL+M_yL_yN_y+M_zL_zN_z+N_y(M_y+L_y)+N_z(M_z+L_z)]$.

The complexity of the single stage: KronF is given by $O[NML]$ and the complexity of the beamforming design given by the TOT method is $O[3M_yL_yN_y+3M_zL_zN_z]$. The total complexity is $O[MNL+3M_yL_yN_y+3M_zL_zN_z]$.

VI. Simulation Results

We consider an IRS-assisted MIMO network where the BS is equipped with $M = 16$ antennas, composed of $M_y = M_z = 4$, and the IRS is equipped with $N = 100$ reflecting elements, composed of $N_y = N_z = 10$ and the UE has $L = 16$ antennas, with $L_y = L_z = 16$. We assume an attenuation of 35 dB and 30 dB on $\boldsymbol{H}$ and $\boldsymbol{G}$, respectively. Also, we consider $\sigma_z^2 = \sigma_a^2 = -80$ dBm. For comparison, the baseline solution is given by the single stage: KRF [7] and the beamforming classical beamforming design [11]. Also, the perfect channel state information (CSI) scenario is used for comparison and the beamforming design is given by the classical solution [11].

Fig. 2 shows the SE varying the pilot power in the channel training stage considering a transmit power $P = 20$ dBm. Due to the processing in the single stage: KronF and the two stage: Kron-KRF part of the noise is rejected and the TOT and KF achieve higher SE compared to the baseline solution. As shown in Fig. 2, the KF and TOT solutions have the same performance since the horizontal and vertical optimization problems in the KF method and in the TOT method are equivalent. Although the TOT requires two estimations, $\hat{\boldsymbol{F}}_y$ and $\hat{\boldsymbol{F}}_z$, it achieves better performance than the classical solution which also requires two estimations, $\hat{\boldsymbol{H}}$ and $\hat{\boldsymbol{G}}$ due to the higher noise rejection in the single stage: KronF when compared to the single stage: KRF. For instance, considering $P_t = 0$ dBm the TOT and the KF have 4 bit/s/Hz more SE compared with the baseline while having 3 bit/s/Hz less SE compared with the perfect CSI.

Fig. 3 shows the SE varying the number of reflecting elements considering pilot power of $P_t = 5$ dBm and transmit power of $P = 20$ dBm. As expected, by increasing the number of reflecting elements the SE of all methods increases due to better channel estimations and higher beamforming gain. Regarding the channel training stage, it is possible to observe a trade-off between the number of reflecting elements and the pilot power in order to achieve a given SE, by increasing the number of reflecting elements the transmitted pilot power

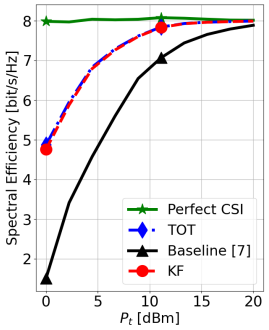

Fig. 2: SE *versus* P_t

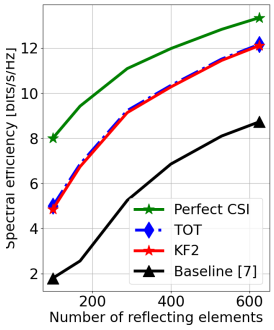

Fig. 3: SE *versus* N

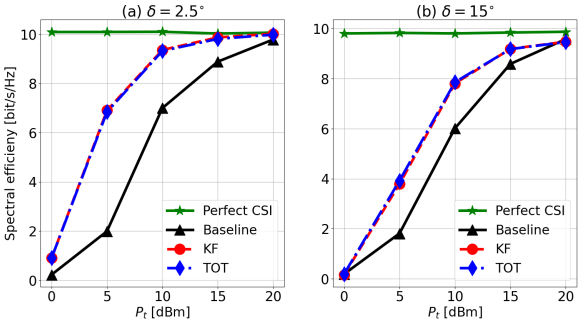

Fig. 4: SE vs P_t for different values of elevation spread

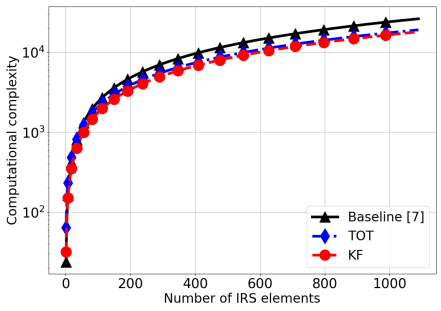

Fig. 5: Computational complexity *versus* N

required to achieve the perfect CSI is reduced. For example, considering 600 reflecting elements, the TOT and KF solutions have 4 bits/s/Hz higher SE than the baseline and it is only 1 bit/s/Hz lower than the perfect CSI case.

In Fig. 4, we consider a scenario where the channels $\boldsymbol{H}$ and $\boldsymbol{G}$ have four paths. The angles of elevation are generated from a uniform distribution $\mathrm{U}[90-\delta, 90+\delta]$, where δ is the elevation spread. As mentioned, for multi-path channels the equations in (8) become approximations and the quality of this approximation is directly associated with the δ. For instance, considering $\delta = 2.5^\circ$, the TOT and KF methods have 3 bit/Hz/s more SE compared with the baseline and for $\delta = 15^\circ$ this gap becomes 1 bit/Hz/S.

Fig. 5 shows the computational complexity of each method varying the number of reflecting elements. The methods which explore the separability of the channels, TOT and KF, present lower computational complexity due to the reduced cost in the joint beamforming design. Considering an IRS with 1000 elements, the TOT and KF methods have, respectively, 37% and 45% less computational complexity than the baseline.

VII. Conclusions

In this paper, we studied the impact of different channel estimation procedures, one method that does not explore the Kronecker factorization structure of the geometrical channels and two methods that explore the Kronecker structure. Once the channel estimation step is done, three beamforming methods, one for each estimation procedure, design the precoder, combiner and IRS phase shifts. The simulation results showed the benefits of exploring the Kronecker structure of the channels in both SE and computational complexity. Perspectives of this work include the extension of the presented channel estimation and beamforming schemes to the joint communication and sensing scenario.

References

[1] E. Basar, M. Di Renzo, J. De Rosny, M. Debbah, M. Alouini, and R. Zhang, "Wireless Communications Through Reconfigurable Intelligent Surfaces," *IEEE Access*, vol. 7, pp. 116 753–116 773, 2019.

[2] S. Gong, X. Lu, D. T. Hoang, D. Niyato, L. Shu, D. I. Kim, and Y.-C. Liang, "Toward smart wireless communications via intelligent reflecting surfaces: A contemporary survey," *IEEE Communications Surveys & Tutorials*, vol. 22, no. 4, pp. 2283–2314, June 2020.

[3] N. A. Abbasi, J. L. Gomez, R. Kondaveti, S. M. Shaikbepari, S. Rao, S. Abu-Surra, G. Xu, J. Zhang, and A. F. Molisch, "Thz band channel measurements and statistical modeling for urban D2D environments," *IEEE Trans. Wireless Commun.*, vol. 22, no. 3, pp. 1466–1479, Mar 2023.

[4] D. Mishra and H. Johansson, "Channel estimation and low-complexity beamforming design for passive intelligent surface assisted miso wireless energy transfer," in *ICASSP 2019 - 2019 IEEE International Conference on Acoustics, Speech and Signal Processing (ICASSP)*, 2019, pp. 4659–4663.

[5] Y. Yang, B. Zheng, S. Zhang, and R. Zhang, "Intelligent reflecting surface meets ofdm: Protocol design and rate maximization," *IEEE Transactions on Communications*, vol. 68, no. 7, pp. 4522–4535, 2020.

[6] T. L. Jensen and E. De Carvalho, "An optimal channel estimation scheme for intelligent reflecting surfaces based on a minimum variance unbiased estimator," in *Proc. ICASSP 2020*, 2020, pp. 5000–5004.

[7] G. T. de Araújo, A. L. F. de Almeida, and R. Boyer, "Channel estimation for intelligent reflecting surface assisted MIMO systems: A tensor modeling approach," *IEEE JSTSP*, vol. 15, no. 3, pp. 789–802, April 2021.

[8] G. T. de Araújo, P. R. B. Gomes, A. L. F. de Almeida, G. Fodor, and B. Makki, "Semi-blind joint channel and symbol estimation in IRS-assisted multiuser MIMO networks," *IEEE Wireless Commun. Lett.*, vol. 11, no. 7, pp. 1553–1557, July 2022.

[9] Fazal-E-Asim, B. Sokal, A. L. F. de Almeida, B. Makki, and G. Fodor, "Tensor-Based High-Resolution Channel Estimation for RIS-Assisted Communications," *arXiv e-prints*, p. arXiv:2304.05576, Apr. 2023.

[10] Fazal-E-Asim, A. L. F. de Almeida, B. Sokal, B. Makki, and G. Fodor, "Two-Dimensional Channel Parameter Estimation for IRS-Assisted Networks," *arXiv e-prints*, p. arXiv:2305.04393, May 2023.

[11] A. Zappone, M. Di Renzo, F. Shams, X. Qian, and M. Debbah, "Overhead-aware design of reconfigurable intelligent surfaces in smart radio environments," *IEEE Trans. Wireless Commun.*, vol. 20, no. 1, pp. 126–141, Jan. 2021.

[12] Y. S. Ribeiro, F. E-Asim, A. L. F. de Almeida, B. Makki, and G. Fodor, "Low-Complexity Joint Active and Passive Beamforming Design for IRS-Assisted MIMO," *arXiv e-prints*, p. arXiv:2305.14650, May 2023.

[13] T. G. Kolda and B. W. Bader, "Tensor decompositions and applications," *SIAM Review*, vol. 51, no. 3, pp. 455–500, 2009.

[14] N. Kishore Kumar and J. Shneider, "Literature survey on low rank approximation of matrices," *arXiv*, p. arXiv:1606.06511, Jun. 2016.